Retrieving Channel Reciprocity for Coordinated Multi-Point Transmission with Joint Processing

Liyan Su, Chenyang Yang, Gang Wang, and Ming Lei

***Abstract*—In time division duplex coordinated multi-point transmission with joint processing (CoMP-JP) systems, the uplink-downlink channels are no longer reciprocal. Due to the difficulty of antenna calibration among the coordinated base stations (BSs), practical downlink channels differ from uplink channels by multiplicative ambiguity factors, which lead to severe performance degradation. In this paper, we propose an inter-BS antenna calibration strategy to facilitate downlink CoMP-JP transmission, whose basic idea is to estimate the ambiguity factors. To establish the observation equations for estimation, an extra uplink training frame except for the regular uplink and downlink frames is introduced, and existing signalling framework of limited feedback can also be reused. To improve the estimation performance, we can either select multiple users or employ multiple frames of one user to assist the calibration. After establishing the observation equations respectively with uplink training or limited feedback, the weighted least square criterion is used for estimation. We proceed to analyze and compare the mean square errors of the estimators, and provide a principle to select the users for assisting calibration. Simulation results show that the channel reciprocity is largely retrieved by the proposed antenna calibration strategy, which provides substantial throughput gain over the CoMP-JP systems without inter-BS calibration.**

***Index Terms*—Coordinated multi-point transmission, channel reciprocity, antenna calibration.**

I. Introduction

COORDINATED multi-point (CoMP) transmission is a spectral-efficient technique for cellular networks, which has attracted extensive research efforts recently [1–5]. When data and channel information can be shared among multiple base stations (BSs), CoMP joint processing (CoMP-JP) is able to fully exploit the potential provided by the network resource [6, 7].

To assist downlink (DL) CoMP-JP multi-user precoding, the global channels of all mobile stations (MSs) should be available at the coordinated BSs. The channel information can be obtained at the BSs via uplink (UL) training in time division duplex (TDD) systems, or by feedback in frequency division duplex (FDD) systems. It is widely recognized that TDD is more applicable for CoMP systems, because large feedback overhead is required in FDD systems to provide the channel information at the BSs [8]. Yet this is established on the assumption of the reciprocity of UL and DL channels.

The global channel of each MS in CoMP systems is a concatenation of multiple single-cell channels. In TDD systems, the global channel is constructed from multiple per-cell channels respectively estimated at the BSs by exploiting the channel reciprocity. However, the UL and DL channels are not reciprocal in practice due to the imperfect calibration on the analog gains of radio frequency (RF) chains in multiple transmit and receive antennas [9,10]. In CoMP-JP systems, the non-ideal channel reciprocity will lead to severe performance degradation [11,12], because it causes a kind of multiplicative noise that will hinder the co-phasing of coherent cooperative transmission. For conciseness, we refer to CoMP-JP as CoMP in the following.

To retrieve the channel reciprocity, antenna calibration is often employed to compensate the mismatch of the RF chains. Self-calibration is a popular antenna calibration method applied in single-cell systems [9], which adjusts all antennas to achieve the same RF analog gain as that of a reference antenna, and hence yields a scalar ambiguity factor between the UL and DL channel vectors. However, self-calibration among BSs is hard to implement in CoMP systems (because coordinated BSs are not co-located). This leads to multiple ambiguity factors between the UL and DL channels at different coordinated BSs. Over-the-air calibration is another method applied in single-cell systems [10, 13], where some users are selected by the BS to assist the calibration, referred to as *calibration supporters* or simply *supporters*. When these users are served as supporters, their UL and DL channels to and from a BS are estimated or quantized to assist antenna calibration, rather than for conveying data as a regular user. To reduce the channel estimation errors for providing accurate calibration, the BS should select a supporter close to the BS. However, in CoMP systems a user close to one BS will be far from another BS. It is not clear how to calibrate the antennas at different BSs with an acceptable performance.

In this paper, we investigate inter-BS antenna calibration strategy for DL CoMP systems, where the ambiguity factors are estimated from the UL and DL channels under weighted least squares (WLS) criterion. To provide observation equations for parameter estimation, we consider two approaches to obtain the UL and DL channels, either via UL training or through limited feedback. We first propose an inter-BS antenna calibration method by exploiting a regular UL training frame, a regular DL training frame and an extra UL training signal weighted by a ratio. We then present a calibration method

Manuscript received May 18, 2013; revised October 20, 2013, January 14 and March 3, 2014. The editor coordinating the review of this paper and approving it for publication was B. Clerckx.

L. Su and C. Yang are with the School of Electronics and Information Engineering, Beihang University, Beijing China (e-mail: liyansu@ee.buaa.edu.cn, cyyang@buaa.edu.cn).

G. Wang and M. Lei are with NEC Laboratories, China (e-mail: {wang_gang, lei_ming}@nec.cn).

Part of this work was published in IEEE WCNC, 2013. This work was supported in part by the National 863 Program 2014AA01A703, and by a research gift from NEC Laboratories, China.

Digital Object Identifier 10.1109/TCOMM.2014.031014.130367

by using the training and feedback frames available in the specification of Long-term Evolution (LTE) [14, 15], which are originally designed for providing the channel direction information (CDI). To reduce the impact of the channel estimation errors, we use the signals received from multiple supporters or from multiple frames of a single supporter. The performance of the proposed methods is analyzed and the principle of selecting supporters is provided.

The rest of this paper is organized as follows. We first present the system mode and formulate the problem in Section II. In Section III, we propose the strategy to estimate the inter-BS ambiguity factor and address several possible variations. In Section IV, we analyze the performance of the proposed estimators and show the principle to select the supporters. Numerical and simulation results are provided in Section V and the paper is concluded in Section VI.

II. System Model and Problem Formulation

Consider a DL cooperative cluster consisting of N_c BSs each equipped with N_t antennas. These BSs cooperatively serve multiple single antenna MSs. Denote $\mathbf{g}_{mb}^D = \sqrt{\alpha_{mb}}\mathbf{h}_{mb}^D \in \mathbb{C}^{1\times N_t}$ as the DL channel vector from BS_b to MS_m, where α_{mb} is the large scale fading gain including path loss and shadowing, $\mathbf{h}_{mb}^D$ is the DL small scale fading channel vector, whose entries are assumed independent and identically distributed (i.i.d.). We assume that the BSs are connected with a central unit (CU) via high capacity backhaul links, and the CU and MSs know perfect large scale fading gains. With the per-cell channel information, $\mathbf{h}_{mb}^D$ and α_{mb}, $b = 1, \cdots, N_c$, the CU constructs the global channel vector of MS_m as $\mathbf{g}_m^D = [\mathbf{g}_{m1}^D \cdots \mathbf{g}_{mN_c}^D]$. After gathering the global channels of all MSs, the CU can compute the multi-cell precoding for DL transmission.

To explain why in TDD systems, the assumption of channel reciprocity does not hold due to the imperfect antenna calibration, we take BS_b and MS_m as an example. As shown in Fig. 1, let S_{bj}^B and Y_{bj}^B denote the transmit and receive analog gains of the jth antenna at BS_b, and S_m^M and Y_m^M denote the transmit and receive analog gains of the antenna at MS_m. Then the UL channel g_{mbj}^U and DL channel g_{mbj}^D between the jth antenna of BS_b and the antenna of MS_m satisfy

$$g_{mbj}^D = \frac{S_{bj}^B Y_m^M}{Y_{bj}^B S_m^M} \cdot g_{mbj}^U \triangleq \beta_{mbj} g_{mbj}^U, \tag{1}$$

where β_{mbj} is a complex ambiguity factor.

As a result, the relationship between the UL and DL per-cell channel vectors can be written as

$$\mathbf{g}_{mb}^D = \mathbf{g}_{mb}^U \cdot \mathbf{B}_{mb}, \tag{2}$$

where $\mathbf{g}_{mb}^U \in \mathbb{C}^{1\times N_t}$ is the UL channel vector from MS_m to BS_b, $\mathbf{B}_{mb} \triangleq \text{diag}\{\beta_{mb1} \cdots \beta_{mbN_t}\}$, and $\text{diag}\{\cdot\}$ stands for a diagonal matrix.

Since without antenna calibration $\beta_{mbi} \neq \beta_{mbj}$ for $i \neq j$, the UL and DL channels are no longer reciprocal.

To retrieve the reciprocity of the per-cell channels, self calibration [13] can be applied. After perfect self-calibration, all antennas at each BS achieve the same RF analog gain as that of a reference antenna. Then, the relationship between the UL and DL channel vectors between BS_b and MS_m becomes

$$\mathbf{g}_{mb}^D = \beta_{mb}\mathbf{g}_{mb}^U. \tag{3}$$

Such a scalar ambiguity factor β_{mb} does not affect the beamforming direction in single-cell single-user systems and hence has no impact on its performance [16].

However, self calibration designed for single-cell systems is not applicable to CoMP systems, where the antennas to be calibrated are not all co-located. On the other hand, even after the perfect self-calibration between each BS and each MS in CoMP systems, the ambiguity factors at different BSs $\beta_{mb}, b = 1, \cdots, N_c$ are not identical. Consequently, the global UL and DL channels are still not reciprocal, which leads to severe performance degradation. This suggests that inter-BS antenna calibration is necessary for CoMP systems. To emphasize the inter-BS antenna calibration and simplify the notation, we assume perfect self-calibration at each BS in the following design and analysis.

Without loss of generality and for notation simplicity, we only calibrate two BSs, say, BS_1 and BS_2. When there are more BSs in the CoMP system, the CU can select one of them as a reference BS and other BSs can calibrate with the reference BS.

After perfect self-calibration, to calibrate BS_1 and BS_2 we only need to estimate the following *inter-BS ambiguity factor*,

$$\mu_{21} \triangleq \frac{\beta_{m2}}{\beta_{m1}} = \frac{S_2^B Y_1^B}{Y_2^B S_1^B}, \tag{4}$$

which only depends on the analog gains at the reference antennas of the two BSs and therefore the subscript i and j for antennas are omitted. Further considering (3) and assuming that the large scale fading gains of UL and DL channels are equal, the factor can be rewritten as,

$$\mu_{21} = \frac{g_{m1j}^U}{g_{m2i}^U}\frac{g_{m2i}^D}{g_{m1j}^D} = \frac{h_{m1j}^U}{h_{m2i}^U}\frac{h_{m2i}^D}{h_{m1j}^D}, i, j = 1, \cdots, N_t, \tag{5}$$

where $h_{mbj}^U = g_{mbj}^U/\sqrt{\alpha_{mb}}$ is the UL small scale fading channel from MS_m to the jth antenna of BS_b.

III. Inter-BS Antenna Calibration Strategy

Previous analysis shows that we can retrieve the global channel reciprocity in CoMP systems by estimating the ambiguity factor between the reference antennas at any two BSs. To do this, it is shown from (5) that the CU needs to obtain both the ratios of UL and DL channels between a supporter and the two BSs, which can be obtained in different ways.

In this section, we present two types of methods to estimate the inter-BS ambiguity factor either via training or via feedback. We first establish the respective observation equations, and derive the statistics of the observation errors. Then, WLS criterion is used to estimate μ_{21}.

To reduce the impact of the imperfect per-cell channels, we can use the signals received from multiple supporters in one frame or from multiple frames of a single supporter. For conciseness, we present the calibration methods by using multiple supporters, and then briefly discuss the methods by using multiple frames.

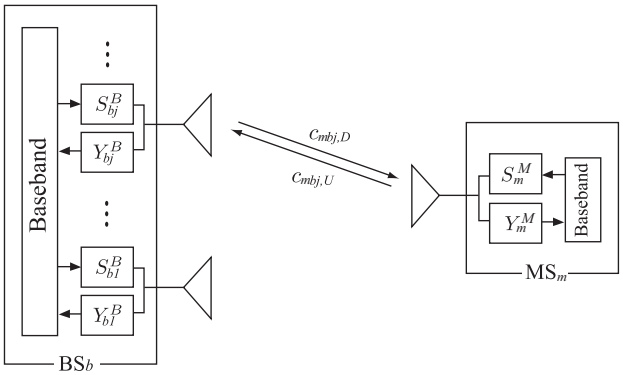

Fig. 1. Illustration of imperfect uplink-downlink channel reciprocity without antenna calibration. Each antenna is equipped with a high power amplifier in the transmitter circuit and a low noise amplifier in the receiver circuit. The UL and DL channels are $g^U_{mbj} = S^M_m c_{mbj,U} Y^B_{b,j}$ and $g^D_{mbj} = S^B_{b,j} c_{mbj,D} Y^M_m$, where $c_{mbj,U}$ and $c_{mbj,D}$ are the UL and DL propagation channels between the antenna pair, which are reciprocal according to electromagnetic theory, i.e. $c_{mbj,U} = c_{mbj,D}$ [9].

A. Inter-BS Antenna Calibration via Training

Suppose that the CU can select several MSs as the supporters to assist calibration, where MS$_m$ located at 1st cell (i.e., BS$_1$ is the master BS of MS$_m$) is one of them.

To obtain the UL and DL channels between the two BSs and the supporters at the CU, we need two UL and one DL training frames.

1) Uplink and Downlink Channel Estimation: In the first UL frame, the supporters send regular training symbols to assist the BSs for channel estimation, each symbol is $\sqrt{p_{UL}}x$ with $|x|^2 = 1$ and p_{UL} is the UL transmit power. To avoid interference among the training signals from multiple MSs, these training symbols are mutually orthogonal. Recall that after perfect self-calibration between each BS and each MS, we only need to calibrate the reference antennas of the BSs, say the first antenna. When linear minimum mean square error (LMMSE) criterion is used for channel estimation, the UL channel from MS$_m$ to the first antenna of BS$_b$ can be expressed by its estimate as

$$g^U_{mb1} = \hat{g}^U_{mb1} + e^U_{mb1}, \qquad b = 1, 2, \tag{6}$$

where $\hat{g}^U_{mb1}$ is the UL channel estimated at BS$_b$, $e^U_{mb1} \sim \mathcal{CN}(0, \varepsilon^U_{mb})$ is the estimation error uncorrelated with the estimated channel,[1] $\varepsilon^U_{mb} = \alpha_{mb}\sigma_U/(\alpha_{mb}p_{UL} + \sigma_U)$, and σ_U is the variance of receiver noise at each BS.

In the DL frame, the BSs broadcast training symbols with transmit power p_{DL}. With the LMMSE channel estimator, the DL channel from the first antenna of BS$_b$ to MS$_m$ can be expressed as

$$g^D_{mb1} = \hat{g}^D_{mb1} + e^D_{mb1}, \qquad b = 1, 2, \tag{7}$$

where $\hat{g}^D_{mb1}$ is the DL channel estimated at MS$_m$, $e^D_{mb1} \sim \mathcal{CN}(0, \varepsilon^D_{mb})$ is the estimation error uncorrelated with the estimated channel, $\varepsilon^D_{mb} = \alpha_{mb}\sigma_D/(\alpha_{mb}p_{DL} + \sigma_D)$, and σ_D is the variance of noise at each MS.

[1]This is valid under the assumption that the user is perfectly synchronized in time and frequency with each BS. Such an assumption is reasonable because in practice the time and frequency mismatch can be significantly reduced by judiciously designed synchronization methods, e.g., [17, 18].

2) Observation Equations for Estimating μ_{21}: With the estimated DL channels, MS$_m$ calculates the ratio of the small scale fading channel of its cross link (i.e., the link from BS$_2$ to MS$_m$) to that of its local link (i.e., the link from its master BS, BS$_1$, to MS$_m$) as follows,

$$\begin{aligned}
\sqrt{\frac{\alpha_{m1}}{\alpha_{m2}}}\frac{\hat{g}^D_{m21}}{\hat{g}^D_{m11}} &= \sqrt{\frac{\alpha_{m1}}{\alpha_{m2}}}\frac{g^D_{m21} + e^D_{m21}}{g^D_{m11} + e^D_{m11}} \\
&= \sqrt{\frac{\alpha_{m1}}{\alpha_{m2}}}\frac{\beta_{m2}g^U_{m21} + e^D_{m21}}{\beta_{m1}g^U_{m11} + e^D_{m11}} \\
&= \sqrt{\frac{\alpha_{m1}}{\alpha_{m2}}}\frac{\mu_{21}g^U_{m21} + e^D_{m21}/\beta_{m1}}{g^U_{m11} + e^D_{m11}/\beta_{m1}} \\
&\triangleq A_m \exp(i\theta_m),
\end{aligned} \tag{8}$$

where A_m and θ_m are the norm and phase of the ratio, respectively, (3) and (4) are used in the derivation.

In the next UL frame, each supporter, say MS$_m$, sends a weighted training symbol $A_m \exp(i\theta_m) \cdot \sqrt{p_{UL}}x$ instead of the regular training symbol, which is referred to as calibration *sounding reference signal (SRS)*. This does not affect the orthogonality of the training signals of multiple supporters. Then, the received calibration SRS at the reference antenna (i.e., the first antenna) of BS$_1$ is

$$z_{m11} = \sqrt{p_{UL}}A_m \exp(i\theta_m)g^U_{m11}x + n^U_1, \tag{9}$$

where n^U_1 is the noise at the BS$_1$.

Substituting (8) into (9) and removing x by multiplying its conjugate, we have

$$\begin{aligned}
\frac{z_{m11}x^*}{\sqrt{p_{UL}}} &= \sqrt{\frac{\alpha_{m1}}{\alpha_{m2}}}\frac{\mu_{21}g^U_{m21} + e^D_{m21}/\beta_{m1}}{g^U_{m11} + e^D_{m11}/\beta_{m1}}g^U_{m11} + \frac{u^U_{11}}{\sqrt{p_{UL}}} \\
&= \sqrt{\frac{\alpha_{m1}}{\alpha_{m2}}}\frac{\mu_{21}g^U_{m21} + e^D_{m21}/\beta_{m1}}{g^U_{m11} + e^D_{m11}/\beta_{m1}} \\
&\quad (g^U_{m11} + e^D_{m11}/\beta_{m1} - e^D_{m11}/\beta_{m1}) + \frac{u^U_{11}}{\sqrt{p_{UL}}} \\
&= \sqrt{\frac{\alpha_{m1}}{\alpha_{m2}}}\mu_{21}g^U_{m21} + v_m,
\end{aligned} \tag{10}$$

where $u^U_{11} = n^U_{11}x^*$, and $v_m = \sqrt{\frac{\alpha_{m1}}{\alpha_{m2}}}\frac{e^D_{m21}}{\beta_{m1}} - \sqrt{\frac{\alpha_{m1}}{\alpha_{m2}}}\frac{\hat{g}^D_{m21}}{\hat{g}^D_{m11}}\frac{e^D_{m11}}{\beta_{m1}} + \frac{u^U_{11}}{\sqrt{p_{UL}}}$.

After the CU collects the UL channel estimates obtained in the first UL frame and the received calibration SRS in the second UL frame from the BS$_1$, it can establish the observation equation for estimating the inter-BS ambiguity factor. Considering (6) and (10), an observation equation for estimating μ_{21} can be obtained as follows

$$\frac{z_{m11}x^*}{\sqrt{p_{UL}}} = \sqrt{\frac{\alpha_{m1}}{\alpha_{m2}}}\mu_{21}\hat{g}^U_{m21} + w_m, \tag{11}$$

where $w_m = \sqrt{\frac{\alpha_{m1}}{\alpha_{m2}}}\mu_{21}e^U_{m21} + v_m$ is the observation noise.

The norms of the ambiguity factors β_{mb} can be modeled as the log-uniformly distributed random variables [19], therefore, $\mathbb{E}\{|\mu_{21}|^2\} = \mathbb{E}\{\frac{1}{|\beta_{mb}|^2}\}^2 \triangleq \bar{\mu}^2 > 1$. Then, the variance of the observation noise can be derived as

$$\begin{aligned}
\epsilon_{T,m} &\triangleq \mathbb{E}\{|w_m|^2\} = \frac{\alpha_{m1}}{\alpha_{m2}}\bar{\mu}^2\varepsilon^U_{m2} + \frac{\alpha_{m1}}{\alpha_{m2}}\bar{\mu}\varepsilon^D_{m2} \\
&+ \frac{1 - \varepsilon^D_{m2}/\alpha_{m2}}{1 - \varepsilon^D_{m1}/\alpha_{m1}}\bar{\mu}\varepsilon^D_{m1} + \frac{\sigma_U}{p_{UL}}.
\end{aligned} \tag{12}$$

After the CU received M_s calibration SRSs, it can obtain M_s observation equations, which is written in a vector form as follows

$$\mathbf{z}_T = \mathbf{u}_T \cdot \mu_{21} + \mathbf{w}_T, \tag{13}$$

where $\mathbf{z}_T = [z_{111}x^*, \cdots, z_{M_s11}x^*]^T/\sqrt{p_{UL}}$, $\mathbf{u}_T = [\sqrt{\frac{\alpha_{11}}{\alpha_{12}}}\hat{g}^U_{121}, \cdots, \sqrt{\frac{\alpha_{M_s1}}{\alpha_{M_s2}}}\hat{g}^U_{M_s21}]^T$,
$\mathbf{w}_T = [w_1, \cdots, w_{M_s}]^T$ is the observation noise with zero mean and covariance matrix

$$\mathbf{R_T} = \mathrm{diag}\{\epsilon_{T,1}, \cdots, \epsilon_{T,M_s}\}. \tag{14}$$

With (13), which is established from one DL training and two different UL training frames of M_s supporters, μ_{21} can be estimated with WLS shown later. We refer to this method as *SRS based multi-supporter calibration (S-MSC)*.

Remark 1: The calibration SRSs can also be sent by the same supporter during M_s DL and $2M_s$ UL frames. The corresponding method is referred to as *SRS based multi-frame calibration (S-MFC)*.

Remark 2: The calibration SRS will change the transmit powers of the UL training signals. To avoid this, MS_m needs to send a normalized calibration SRS, i.e., $\exp(i\theta_m)\cdot\sqrt{p_{UL}}x$. As will be shown in the simulations later, such a normalization leads to a minor performance loss in calibration. By replacing a regular SRS by a normalized calibration SRS, which can also be used to estimate the UL channels, the calibration strategy does not need additional overhead.

B. Inter-BS Antenna Calibration via Limited Feedback

To obtain the UL and DL channels between two BSs and a supporter at the CU, we can also employ one UL training frame, one DL training frame and one feedback frame. In this way, the signalling framework in LTE-A specification [14] can be reused for supporting the inter-BS antenna calibration, where the UL training is served as the *SRS*, the DL training and the succeeded UL feedback aim at reporting CDI to the BS for precoding. In particular, BS_1 obtaining $\hat{\mathbf{g}}^U_{mb}$ and MS_m obtaining $\hat{\mathbf{g}}^D_{mb}$ with the regular UL and DL training shown in III-A1, and the MS conveys the DL CDI to the BS using the regular limited feedback, with which the observation equations for estimating μ_{12} can be established

In [12], another inter-BS antenna calibration method based on limited feedback was proposed, where each supporter estimates the channels from the reference antennas at the two BSs to itself, then combines the two channel coefficients into a vector and feeds back the quantized vector to the CU. The difference of the method presented in this subsection from that in [12] lies in which information is quantized for feedback.

1) Limited Feedback for CDI: After each DL channel is estimated at MS_m, which is $\hat{\mathbf{h}}^D_{mb} = \hat{\mathbf{g}}^D_{mb}/\sqrt{\alpha_{mb}}$, its direction is quantized and fed back to the BS originally used to assist DL beamforming [8]. We consider the *per-cell codebook* based limited feedback for CoMP systems, where MS_m employs single-cell random vector quantization (RVQ) codebooks to separately quantize its per-cell channels $\hat{\mathbf{h}}^D_{mb}, b = 1, 2$, which is tractable for analysis. We assume that the instantaneous norms of per-cell channels $\|\hat{\mathbf{h}}^D_{mb}\|, b = 1, 2$ are perfectly fed back. We consider independent codeword selection [20]. Then, MS_m quantizes its per-cell CDIs as follows,

$$\mathbf{h}^{DF}_{mb} = \arg\max_{\mathbf{c}_i \in \mathcal{C}} \|\bar{\mathbf{h}}^D_{mb}\mathbf{c}_i^H\|, \qquad b = 1, 2, \tag{15}$$

where $\mathcal{C}$ is the per-cell codebook, which consists of unit norm codewords $\mathbf{c}_i \in \mathbb{C}^{1\times N_t}$, $i = 1, \cdots, 2^{B_C}$, B_C is the number of bits to quantize the per-cell CDI and

$$\bar{\mathbf{h}}^D_{mb} = \hat{\mathbf{h}}^D_{mb}/\|\hat{\mathbf{h}}^D_{mb}\| \tag{16}$$

is the per-cell CDI.

With the independent codeword selection, phase ambiguity (PA) $e^{j\phi_{mb}}$ exists, which is a phase rotation between each per-cell CDI and each per-cell codeword. When the PA difference ω_{m2} is fed back with B_P bits using scalar quantization, the negative impact of the PA on CoMP systems can be recovered [8], where the PA differences is $\omega_{mb} \triangleq \phi_{mb} - \phi_{m1}, b = 1, 2$, and $\omega_{m1} = 0$.

After MS_m quantized the per-cell CDIs and the PA difference, it feeds back the indices of the selected codewords to its local BS. Each BS reconstructs the quantized version of the per-channel of MS_m and sends to the CU, which is

$$\mathbf{g}^{DF}_{mb} = \sqrt{\alpha_{mb}}\|\hat{\mathbf{h}}^D_{mb}\|\mathbf{h}^{DF}_{mb}e^{j\hat{\omega}_{mb}}, b = 1, 2, \tag{17}$$

where $\hat{\omega}_{m2}$ is the quantized PA difference.

2) Observation Equations for Estimating μ_{21}: Define $\sin^2\theta_{mb} = 1 - \|\mathbf{h}^{DF}_{mb}(\bar{\mathbf{h}}^D_{mb})^H\|$, which is the per-cell CDI quantization error. Then, the per-cell CDI can be expressed as

$$\bar{\mathbf{h}}^D_{mb} = \cos\theta_{mb}e^{j\phi_{mb}}\mathbf{h}^{DF}_{mb} + \sin\theta_{mb}\mathbf{s}_{mb}, \tag{18}$$

where $\mathbf{s}_{mb} \in \mathbb{C}^{1\times N_t}$ is a unit norm vector isotropically distributed in the null space of $\mathbf{h}^{DF}_{mb}$ [21].

Considering (16), (17), (18) and (7) , the DL per-cell channels can be expressed as

$$\begin{aligned}\mathbf{g}^D_{mb} &= \sqrt{\alpha_{mb}}\|\hat{\mathbf{h}}^D_{mb}\|\bar{\mathbf{h}}^D_{mb} + \mathbf{e}^D_{mb} \\ &= \sqrt{\alpha_{mb}}\|\hat{\mathbf{h}}^D_{mb}\|(\cos\theta_{mb}e^{j\phi_{mb}}\mathbf{h}^{DF}_{mb} + \sin\theta_{mb}\mathbf{s}_{mb}) \\ &= e^{j\phi_{mb_1}}D_{mb}\mathbf{g}^{DF}_{mb} + \mathbf{e}^F_{mb},\end{aligned} \tag{19}$$

where $D_{mb} = \cos\theta_{mb}e^{j\Delta\omega_{mb}}$ is a multiplicative error that comes from the quantization errors of the per-cell CDIs and the PA difference $\Delta\omega_{mb} = \omega_{mb} - \hat{\omega}_{mb}$, and $\mathbf{e}^F_{mb} = \sqrt{\alpha_{mb}}\|\hat{\mathbf{h}}^D_{mb}\|\sin\theta_{mb}\mathbf{s}_{mb} + \mathbf{e}^D_{mb}$ is an additive error that is caused by the quantization error of the per-cell CDIs and DL channel estimation error.

After perfect self-calibration at each individual BS, from (5) the relationship between the UL and DL channels can be expressed as

$$g^D_{m2i}g^U_{m1i} = \mu_{21}g^D_{m1i}g^U_{m2i}, \quad i = 1, \cdots, N_t, \tag{20}$$

which can be written in a matrix form as follows

$$\mathbf{g}^D_{m2}\mathrm{diag}\{\mathbf{g}^U_{m1}\} = \mu_{21}\mathbf{g}^D_{m1}\mathrm{diag}\{\mathbf{g}^U_{m2}\}, \tag{21}$$

where $\mathrm{diag}\{\mathbf{g}^U_{mb}\} = \mathrm{diag}\{g^U_{mb1}, \cdots, g^U_{mbN_t}\}, b = 1, 2$.

Substituting (6) and (19) into (21), N_t observation equations for estimating μ_{21} can be written in a matrix form as

$$\mathbf{g}^{DF}_{m2}\,\mathrm{diag}\{\hat{\mathbf{g}}^U_{m1}\} = \frac{D_{m1}}{D_{m2}}\mathbf{g}^{DF}_{m1}\,\mathrm{diag}\{\hat{\mathbf{g}}^U_{m2}\}\cdot\mu_{21} + \mathbf{w}_m, \tag{22}$$

where $\mathbf{w}_m = \frac{1}{D_{m2}}(\mu_{21}\mathbf{g}_{m1}^{DF}\mathrm{diag}\{\mathbf{e}_{m2}^{U}\}+\mu_{21}\mathbf{e}_{m1}^{F}\mathrm{diag}\{\mathbf{g}_{m2}^{U}\}-\mathbf{g}_{m2}^{DF}\mathrm{diag}\{\mathbf{e}_{m1}^{U}\}-\mathbf{e}_{m2}^{F}\mathrm{diag}\{\mathbf{g}_{m1}^{U}\})$ is the observation noise.

Because the elements of $\mathbf{g}_{mb}^{DF}$, $\mathbf{g}_{mb}^{U}$, $\mathbf{e}_{mb}^{U}$ and $\mathbf{e}_{mb}^{F}$ are i.i.d., the elements of $\mathbf{w}_m$ are also i.i.d.. Therefore, the covariance matrix of the observation noise is

$$\mathbf{R_m} \triangleq \mathbb{E}\{\mathbf{w}_m^H\mathbf{w}_m\} = \epsilon_{F,m}\mathbf{I}_{N_t}, \tag{23}$$

where $\mathbf{I}_{N_t}$ is $N_t \times N_t$ identity matrix.

After the CU collects the UL channel estimates and DL CDIs fed back from M_s supporters, it can estimate the inter-BS ambiguity factor with M_sN_t observation equations, which can be written in a matrix form as follows

$$\mathbf{z}_F = \mathbf{D}_F\mathbf{u}_F \cdot \mu_{21} + \mathbf{w}_F, \tag{24}$$

where $\mathbf{z}_F = [\mathbf{g}_{12}^{F}\mathrm{diag}\{\hat{\mathbf{g}}_{11}^{U}\}\cdots\mathbf{g}_{M_s2}^{F}\mathrm{diag}\{\hat{\mathbf{g}}_{M_s1}^{U}\}]^H$, $\mathbf{D}_F = \mathrm{diag}\{\frac{D_{11}}{D_{12}}\mathbf{I}_{N_t}\cdots\frac{D_{M_s1}}{D_{M_s2}}\mathbf{I}_{N_t}\}$,
$\mathbf{u}_F = [\mathbf{g}_{11}^{DF}\mathrm{diag}\{\hat{\mathbf{g}}_{12}^{U}\}\cdots\mathbf{g}_{M_s1}^{DF}\mathrm{diag}\{\hat{\mathbf{g}}_{M_s2}^{U}\}]^H$, $\mathbf{w}_F = [\mathbf{w}_1\cdots\mathbf{w}_{M_s}]^H$, and the covariance matrix of the observation noise is

$$\mathbf{R_F} = \mathrm{diag}\{\mathbf{R}_1\cdots\mathbf{R}_{M_s}\}. \tag{25}$$

Then, by using WLS, μ_{21} can be estimated. We refer to this method as *CDI based MSC (C-MSC)*.

Remark 3: The CU can also collect the UL channel estimates and DL CDIs fed back from one supporter in M_s UL frames, such a method is referred to as *CDI based MFC (C-MFC)*. In this case, differential quantization [22] can be applied to quantize the CDIs in the multiple frames, such that fewer bits is required to achieve the same quantization accuracy as non-differential quantization.

Remark 4: The multiple supporters can also feed back the ratio $A_m\exp(i\theta_m)$ in (8) after quantizing with a scalar codebook instead of sending the weighted training symbol, in order to establish the observation equations. The corresponding method is referred to as *ratio based MSC (R-MSC)*. Alternatively, the observation equations can be established by allowing one supporter to feed back the ratio in multiple frames using differential quantization. The corresponding method is referred to as *ratio based MFC (R-MFC)*.

C. WLS Estimation

When the large scale fading gains and the receiver noise variances at each BS and each MS are available at the CU, it is shown from the definition of ε_{mb}^{U} and ε_{mb}^{D} in (6) and (7), (12) and (14) that $\mathbf{R_T}$ is known. Similarly, it is shown from the definition of $\mathbf{e}_{mb}^{F}$ in (19), $\mathbf{w}_m$ in (22) and $\mathbf{w}_m^F$ in (24) that $\mathbf{R_F}$ is known.

Note that there is a multiplicative error $\mathbf{D}_F$ in (24) that is unknown at the CU. Without any knowledge of $\mathbf{D}_F$, the CU can simply ignore the error by regarding $\mathbf{D}_F = \mathbf{I}_{M_sN_t}$. This only leads to a minor performance loss, as will be shown in simulations later. Then with the observation equations in (13) or (24) and the corresponding statistics of the observation noises, WLS criterion can be applied to estimate the inter-BS ambiguity factor, which gives rise to

$$\hat{\mu}_{21} = \frac{\mathbf{u}^H\mathbf{R}^{-1}}{\mathbf{u}^H\mathbf{R}^{-1}\mathbf{u}} \cdot \mathbf{z}. \tag{26}$$

For S-MSC, $\hat{\mu}_{21} = \hat{\mu}_{21}^{T}$, $\mathbf{u} = \mathbf{u}_T$, $\mathbf{R} = \mathbf{R_T}$ and $\mathbf{z} = \mathbf{z}_T$. For C-MSC, $\hat{\mu}_{21} = \hat{\mu}_{21}^{F}$, $\mathbf{u} = \mathbf{u}_F$, $\mathbf{R} = \mathbf{R_F}$ and $\mathbf{z} = \mathbf{z}_F$. For all calibration methods using multiple frames, the WLS estimation reduces to the least square estimation, since the observation noises are identical for multiple frames.

Considering that $\mathbf{R}$ is a diagonal matrix, the complexity of the matrix inverse is negligible. As a result, the CU only needs to calculate several additional complex multiplications for the inter-BS calibration. It means that the proposed methods have almost the same complexity as the self-calibration.

D. Procedure of Establishing Observation Equations

For the reader's convenience, the procedures for the two presented calibration methods based on SRS and CDI feedback as well as several possible variations to assist the CU establishing the observation equations are summarized as follows.

- *S-MSC*: 1) each of the multiple supporters sends a regular UL training frame, 2) each BS broadcasts a regular DL training frame, and 3) each supporter sends a calibration SRS.
- *S-MFC*: 1) one supporter sends a regular UL training frame, 2) each BS sends a regular DL training frame, 3) the supporter sends the calibration SRS in next UL frame, and 4) the above steps repeat multiple times.
- *C-MSC*: 1) each of the multiple supporters sends a regular UL training frame, 2) each BS broadcasts a regular DL training frame, and 3) each MS feeds back the quantized DL per-cell CDIs and the PA difference.
- *C-MFC*: 1) one supporter sends a regular UL training frame, 2) each BS sends a regular DL training frame, 3) the supporter feeds back the quantized per-cell CDI and PA difference, and 4) the above three steps repeat multiple times and the CDIs and PA differences in multiple frames are quantized with differential codebooks.
- *R-MSC*: 1) each of the multiple supporters sends a regular UL training frame, 2) each BS broadcasts a regular DL training frame, and 3) each supporter feeds back the ratio of its DL per-cell channels with a scalar codebook.
- *R-MFC*: 1) one supporter sends a regular UL training frame, 2) each BS sends a regular DL training frame, and 3) the supporter feeds back the quantized ratio of its DL per-cell channels, and 4) the above three steps repeat multiple times and the ratios in multiple frames are quantized with differential codebook.

IV. Performance Analysis

In this section, we compare the mean square error (MSE) of the inter-BS ambiguity factor estimation achieved by using the calibration SRS and by reusing the CDI feedback. We also compare the MSEs achieved respectively by using multiple supporters and multiple frames. Based on which, we show how the supporting MSs should be selected.

A. Comparison of the S-MSC, S-MFC and C-MSC

From (13) and (26), the MSE of the inter-BS ambiguity factor estimated with S-MSC or S-MFC is

$$\begin{aligned} & \mathrm{MSE}(\hat{\mu}_{21}^{T}) \\ = \; & \mathbb{E}_{\mathbf{u}_T,\mathbf{w}_T}\{|\mu_{21}-\hat{\mu}_{21}^{T}|^2\} \\ \overset{(a)}{=} \; & \mathbb{E}_{\mathbf{u}_T}\{(\mathbf{u}_T^H {\mathbf{R_T}}^{-1}\mathbf{u}_T)^{-1}\} \\ \overset{(b)}{=} \; & \mathbb{E}_g\{(\sum_{m=1}^{M_s}\frac{\alpha_{m1}|\hat{g}_{m21}^{U}|^2}{\alpha_{m2}\epsilon_{T,m}})^{-1}\} \\ = \; & \mathbb{E}_g\{(\sum_{m=1}^{M_s}\frac{\alpha_{m1}(\alpha_{m2}-\varepsilon_{m2}^{U})}{\alpha_{m2}\epsilon_{T,m}}\frac{|\hat{g}_{m21}^{U}|^2}{\alpha_{m2}-\varepsilon_{m2}^{U}})^{-1}\}, \end{aligned} \quad (27)$$

where (a) is derived after substituting (13) and (26) by using the independence between $\mathbf{u}_T$ and $\mathbf{w}_T$, (b) is obtained by substituting the definition of $\mathbf{u}_T$ in (13) and $\mathbf{R_T}$ in (14).

From (11) it is not hard to show that the first term of (27),

$$\bar{\gamma}_{T,m} \triangleq \frac{\alpha_{m1}(\alpha_{m2}-\varepsilon_{m2}^{U})}{\alpha_{m2}\epsilon_{T,m}} \quad (28)$$

is the average observation signal-to-noise ratio (SNR), and $X_{T,m} \triangleq \frac{\hat{g}_{m21}^{U}}{\sqrt{\alpha_{m2}-\varepsilon_{m2}^{U}}}$ is the normalized channel estimate with unit variance. Then, (27) can be equivalently expressed as

$$\mathrm{MSE}(\hat{\mu}_{21}^{T}) \;=\; \mathbb{E}_X\{(\sum_{m=1}^{M_s}\bar{\gamma}_{T,m}|X_{T,m}|^2)^{-1}\}. \quad (29)$$

Analogous to the derivations for S-MSC and S-MFC, from (24) and (26) the MSE of the inter-BS ambiguity factor estimated with C-MSC can be derived as

$$\begin{aligned} & \mathrm{MSE}(\hat{\mu}_{21}^{F}) = \mathbb{E}_{\mathbf{u}_F,\mathbf{w}_F}\{|\mu_{21}-\hat{\mu}_{21}^{F}|^2\} \\ \overset{(c)}{=} \; & \mathbb{E}\{|\frac{\mathbf{u}_F^H {\mathbf{R_F}}^{-1}\mathbf{w}_F}{\mathbf{u}_F^H {\mathbf{R_F}}^{-1}\mathbf{u}_F}|^2+|1-\frac{\mathbf{u}_F^H {\mathbf{R_F}}^{-1}\mathbf{D}_F\mathbf{u}_F}{\mathbf{u}_F^H {\mathbf{R_F}}^{-1}\mathbf{u}_F}|^2|\mu_{21}|^2\}, \end{aligned} \quad (30)$$

where (c) is derived by substituting (24) and (26). The second term of the MSE comes from treating $\mathbf{D}_F$ as $\mathbf{I}_{M_s N_t}$ in the WLS estimator.

The following proposition provides the MSE lower bounds of the S-MSC, S-MFC and C-MSC, considering that in practice the number of supporters or frames, M_s, will be finite.

Prop. 1: When $M_s \to \infty$, the MSEs of S-MSC and S-MFC converge to zero, i.e.,

$$\lim_{M_s\to\infty}\mathrm{MSE}(\hat{\mu}_{21}^{T}) = 0, \quad (31)$$

and the MSE of C-MSC converges to a positive constant, i.e.,

$$\lim_{M_s\to\infty}\mathrm{MSE}(\hat{\mu}_{21}^{F}) = \psi^2+\bar{\mu}^2(1-\Phi\cdot\frac{\sin(2^{-B_P}\pi)}{2^{-B_P}\pi})^2, \quad (32)$$

where $\psi \triangleq |\frac{\mathbb{E}\{(\mathbf{g}_{m1}^{DF}\,\mathrm{diag}\{\hat{\mathbf{g}}_{m2}^{U}\}\epsilon_{F,m}^{-1}\mathbf{w}_m^H)\}}{N_t\mathbb{E}\{\bar{\gamma}_{F,m}|X_{F,m,n}|^2\}}|$, $\Phi \triangleq \frac{\mathbb{E}\{\bar{\gamma}_{F,m}|X_{F,m,n}|^2\frac{\cos\theta_{m1}}{\cos\theta_{m2}}\}}{\mathbb{E}\{\bar{\gamma}_{F,m}|X_{F,m,n}|^2\}}$ depends on the number of bits used to quantize the per-cell CDI and the average observation SNR, $\bar{\gamma}_{F,m} \triangleq \frac{(\alpha_{m1}-\varepsilon_{m1}^{D})(\alpha_{m2}-\varepsilon_{m2}^{U})}{\epsilon_{F,m}}$ is the average observation SNR of each scalar equation in (22), and $X_{F,m,n} \triangleq \frac{g_{m1n}^{F}\hat{g}_{m2n}^{U}}{\sqrt{(\alpha_{m1}-\varepsilon_{m1}^{D})(\alpha_{m2}-\varepsilon_{m2}^{U})}}$.

Proof: See Appendix A.

Note that ψ, Φ and $\frac{\sin(2^{-B_P}\pi)}{2^{-B_P}\pi}$ reflect the impact of the quantization error of the per-cell CDIs and PA difference. The proposition suggests that the calibration performance of the C-MSC will be limited by the number of bits for feedback, even when we are able to employ a large number of supporters for the calibration. Considering that the number of bits for feedback can not be large in practice, the C-MSC will preform much worse than S-MSC and S-MFC, as will be shown from the simulations later. Therefore, in the sequel, we will no longer discuss the C-MSC.

Now we proceed to compare the performance of the S-MSC and S-MFC. (29) can be rewritten in a matrix form as follows

$$\mathrm{MSE}(\hat{\mu}_{21}^{T}) \;=\; \mathbb{E}_{\mathbf{X}}\{(\mathbf{X}^H\bar{\mathbf{\Gamma}}\mathbf{X})^{-1}\}, \quad (33)$$

where $\bar{\mathbf{\Gamma}} \triangleq \mathrm{diag}\{\bar{\gamma}_{T,1}\cdots\bar{\gamma}_{T,M_s}\}$, $\mathbf{X} = [X_{T,1}\cdots X_{T,M_s}]^H$ is a random vector of complex Gaussian distribution with zero mean and covariance matrix $\mathbf{\Phi_X}$, and the diagonal elements of $\mathbf{\Phi_X}$ are equal to 1 that are the variances of $X_{T,m}$, $m = 1,\cdots,M_s$.

The channels of multiple MSs are usually independent, but the channels in multiple frames of one MS may be correlated in general. As a result, when using the S-MSC, $\mathbf{\Phi_X} = \mathbf{I}_{M_s}$. When using the S-MFC, the off-diagonal elements of $\mathbf{\Phi_X}$ may not be equal to zero due to the correlation of the channels in $\mathbf{u}_T$ defined in (13).

For a fair comparison, we consider that the average observation SNRs of the observation equations for different calibration methods are all equal to $\bar{\gamma}$, i.e., $\bar{\mathbf{\Gamma}} = \bar{\gamma}\cdot\mathbf{I}_{M_s}$. Then, we can rewrite (27) as

$$\mathrm{MSE}(\hat{\mu}_{21}^{T}) = \mathbb{E}_{\mathbf{X}}\{(\bar{\gamma}\mathbf{X}^H\mathbf{X})^{-1}\}. \quad (34)$$

Because $\mathbf{\Phi_X} = \mathbf{I}_{M_s}$ when using the S-MSC, and the covariance matrix is not an identity matrix when using the S-MFC, the following proposition implies that the S-MSC outperforms the S-MFC.

Prop. 2: The MSE of the inter-BS ambiguity factor estimate achieves its minimum if and only if $\mathbf{\Phi_X} = \mathbf{I}$.

Proof: See Appendix B.

B. Selection of Calibration Supporters

From (33) we can see that the MSE depends on the number of supporters or frames M_s, the covariance matrix $\mathbf{\Phi_X}$ and the average observation SNR $\bar{\gamma}_{T,m}$. This suggests that the following means can be applied to improve the calibration performance, since the CU can gather all the required information to establish the observation equations and then estimate the ambiguity factors. 1) The CU can use S-MSC by selecting more supporters when there are large number of active MSs. Otherwise, the CU can employ the S-MFC with large number of frames from one supporter. Recall that the supporter assisting S-MSC or S-MFC acts differently as summarized in the calibration procedure in section III.D. 2) The CU selects appropriate supporters to increase the average observation SNR.

From the definition of $\bar{\gamma}_{T,m}$ in (28), we can see that it depends on the location of the supporters. In the following proposition, we show how the supporters should be selected to optimize the calibration performance.

We first define two notions to be used. When MS_m is located at the "exact cell-edge", we mean all the large scale fading gains of the user are equal, i.e., $\alpha_1 = \cdots = \alpha_{N_c}$.[2] For a MS with distance r from its master BS, its average DL receive SNR is called *cell-edge SNR*, where r is the cell radius. To reflect the impact of the inter-cluster interference, the interference power can be included in the noise power.

Prop. 3: When a system has high cell-edge SNR, the optimal location of the supporters that maximizes the average observation SNR is the exact cell-edge.

Proof: Upon substituting (12), the average observation SNR can be obtained as

$$\bar{\gamma}_{T,m} = \frac{\alpha_{m1}(\alpha_{m2} - \varepsilon^U_{m2})}{\alpha_{m1}(\bar{\mu}^2\varepsilon^U_{m2} + \bar{\mu}\varepsilon^D_{m2}) + \alpha_{m2}(\frac{1-\varepsilon^D_{m2}/\alpha_{m2}}{1-\varepsilon^D_{m1}/\alpha_{m1}}\bar{\mu}\varepsilon^D_{m1} + \frac{\sigma_U}{p_{UL}})}, \tag{35}$$

where $\bar{\mu}$ is defined before (12).

When the cell-edge SNR is high, $\alpha_{mb}p_{UL} \gg \sigma_U$. From the definition of ε^U_{mb} after (6), we can see that its denominator is dominated by $\alpha_{mb}p_{UL}$. Thus, we have $\varepsilon^U_{mb} \approx \sigma_U/p_{UL}$. For the same reason, $\varepsilon^D_{mb} \approx \sigma_D/p_{DL}$. Then, (35) can be approximated as

$$\begin{aligned}\bar{\gamma}_{T,m} &\approx (\frac{\bar{\mu}^2\sigma_U}{p_{UL}\alpha_{m2}} + \frac{\bar{\mu}\sigma_D}{p_{DL}\alpha_{m2}} + \frac{\bar{\mu}\sigma_D}{p_{DL}\alpha_{m1}} + \frac{\sigma_U}{p_{UL}\alpha_{m1}})^{-1} \\ &= \frac{1}{4}\cdot\frac{4}{(\frac{\gamma^U_{m2}}{\bar{\mu}^2})^{-1} + (\frac{\gamma^D_{m2}}{\bar{\mu}})^{-1} + (\frac{\gamma^D_{m1}}{\bar{\mu}})^{-1} + (\gamma^U_{m1})^{-1}},\end{aligned} \tag{36}$$

which is a harmonic mean multiplied by a constant, where γ^U_{mb} and γ^D_{mb} are the UL and DL SNRs of the received signals at BS_b and at MS_m, respectively.

Note that $\bar{\mu} > 1$, and in practical systems, the SNR of local link (i.e., the link from the master BS of MS_m, BS_1, to MS_m) is higher than that of cross link (i.e., the link from BS_2 to MS_m), because the local link have higher channel gain. As a result, the MSE is dominated by the minimum term, i.e.,$\gamma^U_{m2}/\bar{\mu}^2$ or $\gamma^D_{m2}/\bar{\mu}$, where γ^U_{m2} and γ^D_{m2} are the UL and DL SNRs of the cross link, respectively. It implies that in order to reduce the observation errors, cell-edge MSs should be selected to assist the inter-BS calibration. As shown in simulations later, this conclusion is still valid when the cell-edge SNR is not high.

V. Numerical and Simulation Results

In this section we validate previous analytical analysis and evaluate the performance of several inter-BS antenna calibration methods via simulations.

A. Simulation Setting

In the simulation, we consider hexagon cells, the radius of each cell $r = 250$ m. Each BS transmits with a maximal power of 46 dBm, and each MS transmits with a maximal power of 23 dBm. The path loss exponent is 3.76, and the minimum BS-MS distance is 35 m. These simulation parameters are from [23]. Sectorized antenna patterns and shadowing are not considered. The receiver noise floor of BS is -116.4 dBm, and that of MS is -97.5 dBm [24].

Unless otherwise specified, we consider the following setting in all of the simulations.

- Three neighboring BSs are cooperated. All the MSs are randomly distributed in a "x dB edge region", e.g., the value of $\alpha_{mb_m}/\sum_{b\neq b_m}\alpha_{mb}$ is less than x dB for MS_m. When the distance between MS and its local BS is d, its DL SNR is $\text{SNR}_c + 37.6\log_{10}(r/d)$, where SNR_c is the ratio of average receive power to noise variance for a user exactly with distance r from the BS, denoted as cell-edge SNR, which is used as a control parameter to change the bias points of the simulations. We model the inter-cluster interference as white Gaussian noise, which is the worst case interference and results in pessimistic performance [25]. Consequently, inter-cluster interference is implicitly reflected in SNR_c. We set SNR_c as 10 dB, corresponding to a particular channel and deployment scenario. The simulation results are obtained from 100 small scale channel realizations with i.i.d. Rayleigh fading and 200 random locations of the MSs.
- We consider a realistic scenario where the self-calibration within each BS is imperfect, such that β_{mbj} defined in (1) is not equal to β_{mb} in (3). Different values of β_{mbj}/β_{mb} are assumed to be independent, their norms are modeled as a log-uniformly random variable distributed within $[-1, 1]$ dB, and their phases are modeled as a random variable uniformly distributed in $[-10°, 10°]$ [19]. The ambiguity factors of the reference antenna in different BSs, β_{mb}, are independent, whose norms are modeled as a log-uniformly random variable distributed within $[-3, 3]$ dB, and the phases are modeled as random variable a uniformly distributed within $[-180°, 180°]$.
- For all the methods using multiple supporters, the CU randomly selects 30 MSs as the supporters. For all the methods using multiple frames, we consider a realistic time-varying channel model, Jakes Model, which is widely applied [26]. The duration of each UL or DL frame is 10 ms. For the R-MSC, the norm and phase of the ratio $A_m\exp(i\theta_m)$ are fed back with 4 bits, respectively. For the C-MSC, Grassmannian line packing (GLP) codebook is used to quantize the per-cell CDIs, which is optimal for i.i.d. channels [27]. Each per-cell CDI and each PA difference are fed back with 4 bits, respectively.

B. Validation of the Analytical Results

To validate the asymptotic results in *proposition 1* and the approximated results in *proposition 3*, in Fig. 2 we compare the simulated MSE with finite number of supporters under realistic cell-edge SNR with the numerical results. Since in the analysis RVQ codebook is considered, in this simulation we also use this codebook. From Fig. 2(a) we can see that the simulated MSE of the C-MSC converges to the asymptotic result (obtained from (32)) faster than that of the S-MSC (whose asymptotic result is obtained from (31)). This is

[2]Note that this is a mathematical definition to facilitate analysis. In practice, when considering the path loss, shadowing and sector antenna power gains, such a user may rarely appear.

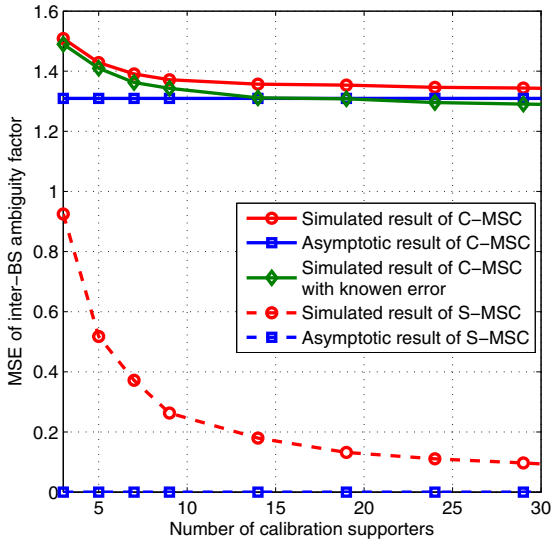

(a) Simulation and asymptotic results of the MSEs of the S-MSC and C-MSC. The supporters are located at exact cell-edge.

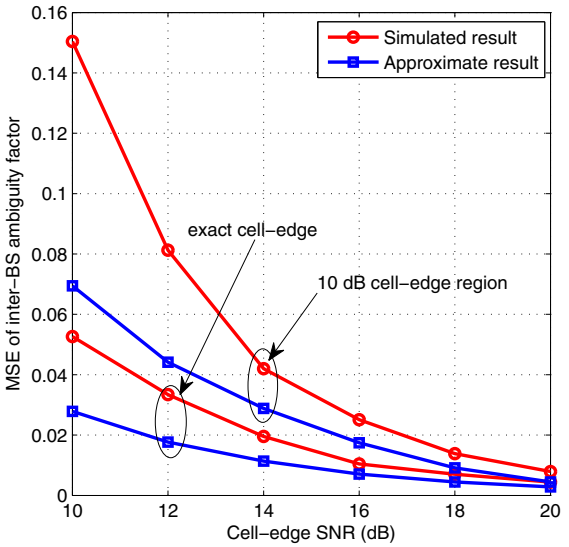

(b) Simulation and approximated results of the MSE of the S-MSC.

Fig. 2. Simulation and numerical results of the MSEs of S-MSC and C-MSC.

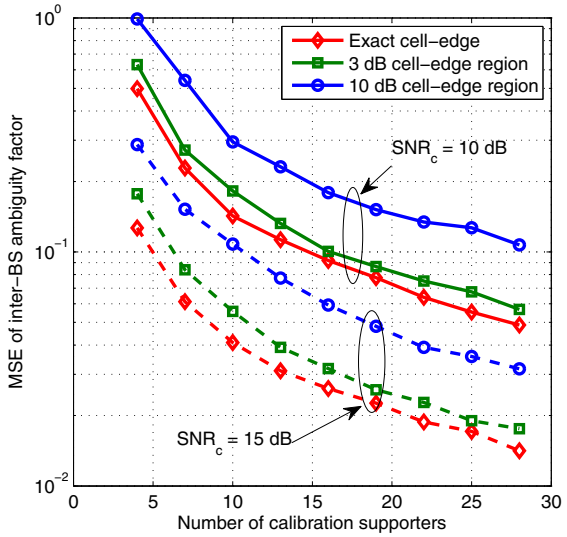

(a) MSE of the inter-BS ambiguity factor estimation

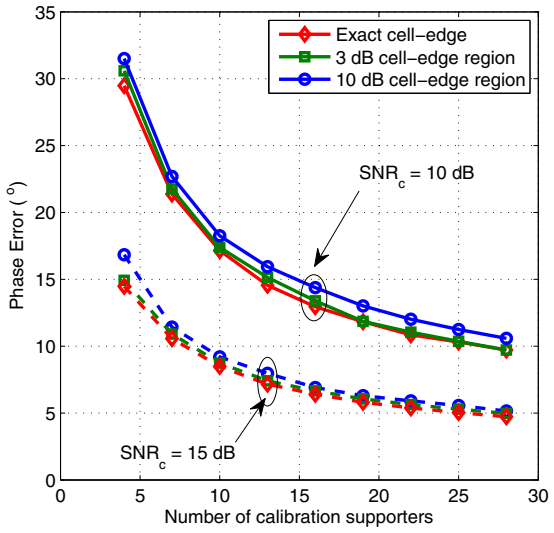

(b) Phase error of the inter-BS ambiguity factor estimation

Fig. 3. MSE and phase error of the inter-BS ambiguity factor estimated with the S-MSC.

because the number of scalar observation equations of C-MSC is $N_t M_s$, while that of S-MSC is M_s. However, the MSE of C-MSC is much higher than the MSE of S-MSC, since the number of bits for feedback is limited. To show the impact of simply setting the unknown multiplicative error $\mathbf{D}_F$ as identity matrix, we provide the simulation result when $\mathbf{D}_F$ is known. We can see that the knowledge of $\mathbf{D}_F$ only improves the performance slightly. The approximated results in Fig. 2(b) is obtained from (29), where the observation SNR $\bar{\gamma}_{T,m}$ is calculated from (36). We can see that the simulation results converge to the approximated results at high cell-edge SNR.

In Fig. 3 we show the MSE and phase error (defined as $\mathbb{E}\{|\arg(\hat{\mu}_{21}) - \arg(\mu_{21})|\}$, $\arg(z)$ stand for the phase of z) of the inter-BS ambiguity factor estimated with the S-MSC. We can see that the supporters located at the exact cell-edge provides the best performance, which agrees with the conclusion in *proposition 2*. We can also see that the conclusions obtained for MSE analysis are also valid for phase error, but the phase error of the estimation is not sensitive to the location of the supporters.

C. Performance Comparison of the Calibration Methods

In Fig. 4, we compare the MSEs of three calibration methods using multiple supporters when the number of supporters M_s or the number of feedback bits of each user in the C-MSC and R-MSC increases. In R-MSC, the number of bits for quantizing the norm and phase of the ratio are identical (e.g., 8 bits for a user means 4 bits for the norm and 4 bits for the phase). In C-MSC, the number of bits for quantizing

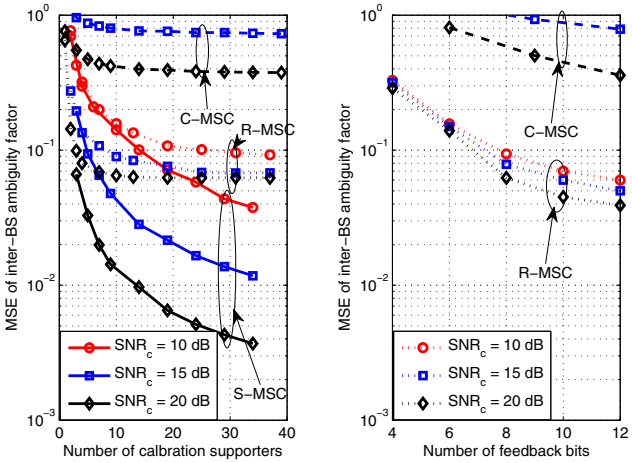

(a) MSE versus M_s, the number of feedback bits per-user is 8 bits in R-MSC, and 12 bits in C-MSC.

(b) MSE versus the number of feedback bits per-user, $M_s = 30$

Fig. 4. Comparison of several calibration methods using multiple supporters, which are located at exact cell-edge.

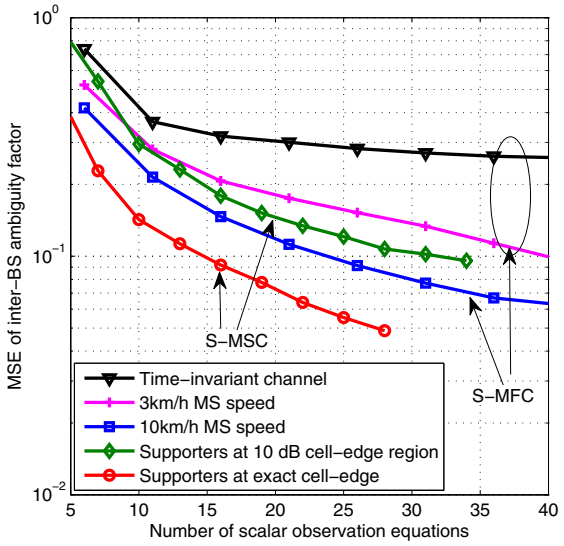

Fig. 5. Comparison of the calibration methods using multiple supporters and multiple frames.

each per-cell CDI and PA difference feedback are identical (e.g., 9 bits for a users means 3 bits for each per-cell CDI and 3 bits for the PA difference). As shown in Fig. 4(a), the MSE of the proposed S-MSC reduces rapidly with the number of supporters, while the MSEs of the other two methods are severely limited by the quantization error. To achieve the same MSE, the S-MSC needs much less supporters than the R-MSC. As shown in Fig. 4(b), the MSEs achieved by the R-MSC and C-MSC reduce with the increase of the number of bits for feedback. The R-MSC outperforms the C-MSC. However, when each user employs 12 bits, the R-MSC is still much worse than the S-MSC. In this case, overall $12M_s = 360$ bits are feedback, which is indeed a large number. When more bits are used, a MSE floor will appear for both C-MSC and R-MSC, which is not shown in the figure.

In Fig. 5 we compare the MSEs of the inter-BS ambiguity factor estimated with the S-MSC and the S-MFC, given the same number of observation functions (i.e., the number of supporters in MSC, and the repeated times of the multiple steps in S-MFC). For the S-MFC, a supporter is located at the exact cell edge and moves at different speeds of 0 km/h, 3 km/h and 10 km/h, where the carrier frequency is 2 GHz. We can see that the MSE of the S-MFC decreases when the speed of the supporter increases. This is because the coherence time decreases with the MS's speed, and the covariance matrix $\mathbf{\Phi_X}$ approaches to $\mathbf{I}_{M_s}$ when the coherence time is close to zero. Furthermore, the MSE of the S-MSC decreases much faster than that of the S-MFC. We can also see that even when the supporters are located within a 10 dB edge region, the S-MSC still outperforms the S-MFC with a low speed supporter.

In Fig. 6 we compare the MSEs achieved by several calibration methods based on limited feedback, given the same number of observation functions (i.e., the number of feedback frames in C-MFC and R-MFC). Unless explained in the legend, time-invariant channel is considered and the supporters are located in the exact cell edge. When using the

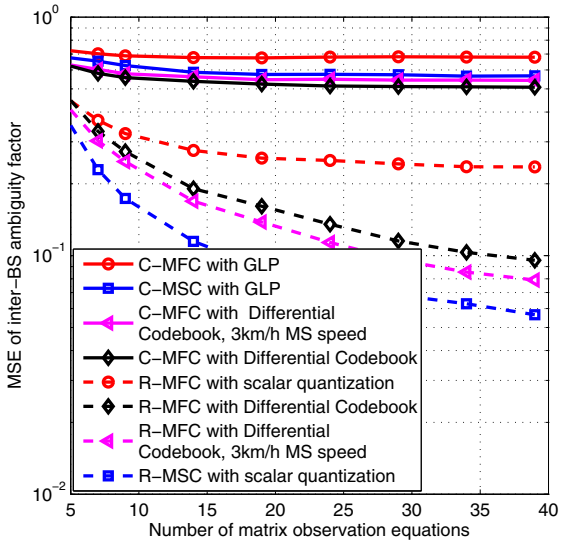

Fig. 6. Comparison of the calibration methods based on limited feedback.

GLP and differential codebook [22], each per-cell CDI and PA difference are fed back with 4 bits, respectively. When using the scalar quantization and scalar differential quantization, the norm and phase of the ratio are fed back with 4 bits, respectively. In the scalar quantization, uniform quantization of the norm (from -20 dB to 20 dB) and phase (from $-\pi$ to π) is considered. In the scalar differential quantization, we employ a method similar to that presented in [28]. From the figure we can see that using differential quantization for the calibration methods with multiple frames can improve the performance, and the gain for R-MFC is more significant. When the supporter moves with 3 km/h, the MSE achieved by R-MFC further reduces, but is still higher than the R-MSC. This result seems inconsistent with the intuition that differ-

ential codebook achieves the highest feedback accuracy when the MS does not move. Yet this intuition is only true when we quantize CDI, while in R-MFC the ratio $A_m \exp(i\theta_m)$ is quantized, which does not have a direct relation with channel variation. Moreover, we have shown in Fig. 5 that MFC has a better performance when MS moves faster, which dominates the MSE of the ambiguity factor estimate. On the other hand, the MSE does not decrease with the number of observations for C-MFC with differential codebook even when the MS is stationary. Such an unexpected result is caused by the selected differential codebook. Other type of differential codebooks may not show such a saturation and may provide a lower MSE. A comprehensive comparison of differential codebooks optimized for inter-BS antenna calibration is for further study. Comparing Fig. 5 and Fig. 6, we can find that the R-MSC is inferior to the S-MSC.

D. Impact of the Inter-BS Calibration on DL Achievable Rate

To show the impact of the inter-BS calibration on the DL transmission performance, we simulate the average achievable data rate of each user, where three cooperative BSs each equipped with four antennas cooperatively serve three MSs. We consider zero-forcing (ZF) precoding both for CoMP and non-CoMP systems. In CoMP systems, ZF precoding consists of ZF beamforming and an optimal power allocation that maximizes the sum rate under the per-BS power constraint (PBPC) [29]. The DL achievable rate is computed by Shannon capacity formula.

In Fig. 7 we show the average per-user rate when the following methods are applied. All the MSs and calibration supporters are randomly distributed in a 3 dB edge region. Note that the receive SNRs of these supporters may be higher than the cell-edge SNR (the x-axis) because they are randomly located.

1) Perfect calibration: the CU knows error-free inter-BS ambiguity factors μ_{i1}, $i = 2, 3$.
2) Perfect phase calibration: the CU knows error-free phases of μ_{ij}, i.e., $\arg(\mu_{ij})$.
3) S-MSC: the supporters send the calibration SRS without normalization, $A_m \exp(i\theta_m) \cdot x$.
4) S-MSC with normalized SRS: the supporters send the calibration SRS with normalization, $\exp(i\theta_m) \cdot x$.
5) R-MSC: each of the supporters feed back 4 bits for uniformly quantizing the norm and 4 bits for the phase of $A_m \exp(i\theta_m) \cdot x$.
6) C-MSC: each of the supporters feed back 4 bits for each per-cell CDI and 4 bits for each PA difference.
7) FDD systems: 4 bits are used for quantizing each per-cell CDI and for quantizing each phase ambiguity (PA) difference, respectively. Then the quantized global CDI is reconstructed at the CU and used for DL precoding [20].
8) Perfect self-calibration: CoMP with perfect self-calibration but without inter-BS calibration.
9) Non-CoMP: three BSs transmit to the users in their own cells without cooperation.
10) Method in [12]: the inter-BS calibration method proposed in [12].

To show how the MSE of the ambiguity factor estimation translates to the rate loss of CoMP systems, we provide some typical MSE values of several schemes. It is shown that the achievable rate gap between the perfect calibration and the perfect self-calibration-only method is large, which is caused by the inter-BS ambiguity factors. Without the inter-BS calibration, CoMP will become inferior to non-CoMP. The S-MSC without normalized SRS performs closely to the perfect calibration, and the S-MSC with normalized SRS performs close to the perfect phase calibration. When the R-MSC is used, the performance is always worse than that of the S-MSC without normalized SRS, but is a little bit better than the S-MSC with normalized SRS for high cell-edge SNR. By comparing the performance between the perfect calibration and the perfect phase calibration, we can see that the performance loss is dominated by the phase of μ_{ij}. This is because only the multi-user interference (MUI) depends on the norm of ambiguity factor, but both the signal and MUI depend on the phase ambiguity. As anticipated, the C-MSC performs the worst among all the inter-BS calibration methods. In FDD systems, the antennas do not need to calibrate, but the performance is destroyed by the quantization errors of CDI and PA. Comparing Fig. 7(a) and Fig. 7(b), we can see that the S-MSC outperforms the R-MSC, both outperform the method in [12].

In LTE systems, only finite number of orthogonal SRS are available. In Fig. 8, we show the impact of the non-orthogonal SRS on the average per-user achievable rate, where all the MSs and calibration supporters are randomly distributed in a 3 or 10 dB cell edge region or whole cell, and the training sequences for the supporters and MSs in different cells are nonorthogonal as generated in [30]. It is shown that when the MSs are located in the cell edge region, the non-orthogonal SRS leads to minor performance degradation. This is because during the UL training the interference from other cells are much lower than the receiver noise.

In summary, the evaluation results suggest that the S-MSC is the best calibration method when there are multiple supporters to be selected in practice. If only one MS is able to assist the calibration, the S-MFC will perform well when the channel of the MS is in fast fading. If the feedback overhead is not a concern, the R-MSC performs close to the S-MSC at high cell-edge SNR. Finally, if the training and feedback frames in LTE specification are not allowed to revise for supporting the inter-BS calibration, the C-MSC is a solution but the performance is not good.

VI. Conclusion

In this paper, we studied inter-BS antenna calibration strategy to alleviate the performance degradation caused by the non-ideal uplink-downlink channel reciprocity in DL TDD CoMP systems. The strategy can be implemented either with multiple supporters or with multiple uplink frames from a single supporter, and either with a calibration SRS or with feedback. We analyzed the performance of typical methods, and provided the principle to select the users assisting calibration. Both analytical and simulation results showed that cell-edge users should be selected to assist the inter-BS antenna calibration. In general, the calibration with multiple supporters

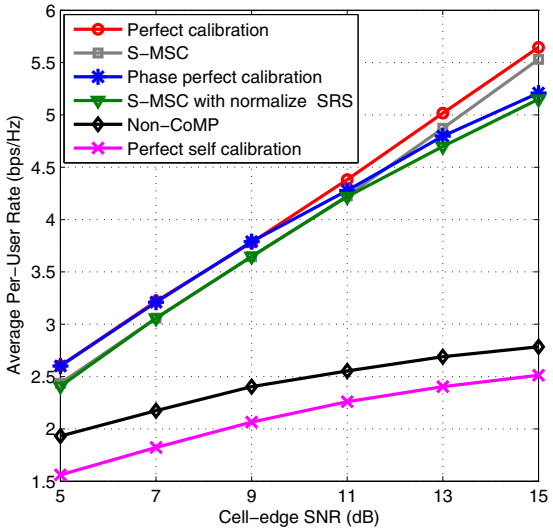

(a) Performance of training based calibrations

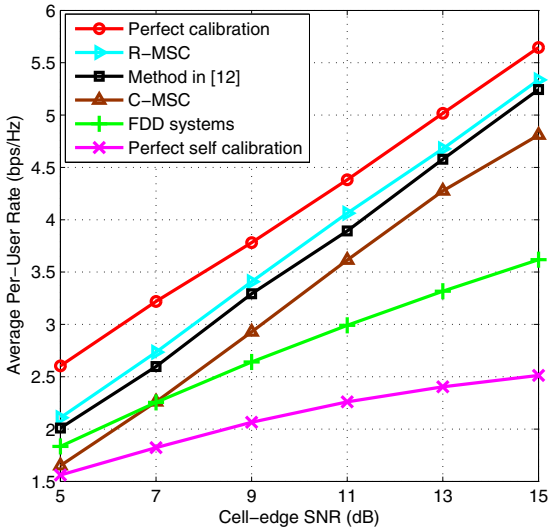

(b) Performance of quantization based calibrations

Fig. 7. Average per-user achievable data rate with different antenna calibration methods. When cell-edge SNR is 10 dB, the MSEs of S-MSC, R-MSC and C-MSC are $5 \times 10^{-2}, 9 \times 10^{-2}$ and 1.1 respectively.

outperforms the calibration with multiple frames from one low-mobility supporter. The proposed method of sending calibration SRS performs the best with a few supporters. The average data rate achieved by each user increases significantly by using the proposed inter-BS calibration method, which is close to that with perfect calibration.

Appendix A
Proof of Prop.1

When the number of supporters $M_s \to \infty$, the MSE of S-MSC or S-MFC is

$$\lim_{M_s\to\infty} \text{MSE}(\hat{\mu}_{21}^T) = \lim_{M_s\to\infty} \frac{1}{M_s}\mathbb{E}_X\{(\frac{1}{M_s}\sum_{m=1}^{M_s}\bar{\gamma}_{T,m}|X_{T,m}|^2)^{-1}\}. \quad \text{(A.1)}$$

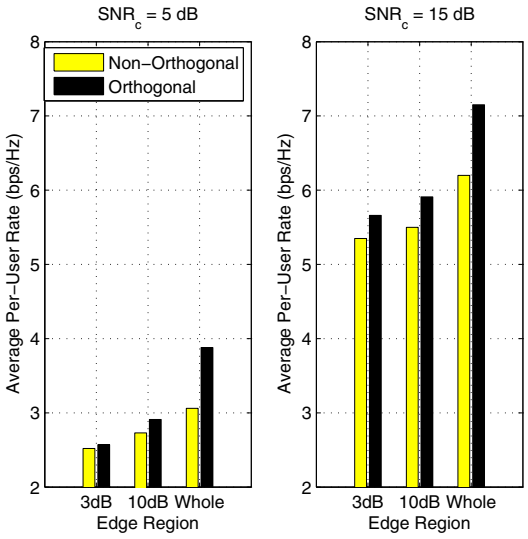

Fig. 8. Average per-user achievable data rate with orthogonal or non-orthogonal SRS.

Because $\bar{\gamma}_{T,m}|X_{T,m}|^2, m = 1, \cdots, M_s$ are independent, from the law of large numbers we obtain

$$\lim_{M_s\to\infty} \frac{1}{M_s}\sum_{m=1}^{M_s}\bar{\gamma}_{T,m}|X_{T,m}|^2 = \mathbb{E}_X\{\bar{\gamma}_{T,m}|X_{T,m}|^2\}, \quad \text{(A.2)}$$

which is is a constant not depending on M_s.

Substituting (A.2) into (A.1) and further considering (23), we have

$$\lim_{M_s\to\infty} \text{MSE}(\hat{\mu}_{21}^T) = \lim_{M_s\to\infty} \frac{(\mathbb{E}_X\{\bar{\gamma}_{T,m}|X_{T,m}|^2\})^{-1}}{M_s} = 0.$$

This proves (31). In the sequel, we prove (32) for the C-MSC.

From the definition of $\mathbf{u}_F$ in (24) and $\mathbf{R_F}$ in (25), we have

$$\mathbf{u}_F^H {\mathbf{R_F}}^{-1}\mathbf{u}_F = \sum_{m=1}^{M_s}(\bar{\gamma}_{F,m}\sum_{n=1}^{N_t}|X_{F,m,n}|^2). \quad \text{(A.3)}$$

Substituting (A.3) into the first and second terms in (30) and further considering (23), we obtain

$$\begin{aligned}
&\mathbb{E}\{|\frac{\mathbf{u}_F^H {\mathbf{R_F}}^{-1}\mathbf{w}_F}{\mathbf{u}_F^H {\mathbf{R_F}}^{-1}\mathbf{u}_F}|^2\} \\
=\ &\mathbb{E}\{|\frac{\sum_{m=1}^{M_s}(\mathbf{g}_{m1}^{DF}\text{diag}\{\hat{\mathbf{g}}_{m2}^U\}\epsilon_{F,m}^{-1}\mathbf{w}_m^H)}{\sum_{m=1}^{M_s}(\bar{\gamma}_{F,m}\sum_{n=1}^{N_t}|X_{F,m,n}|^2)}|^2\} \\
=\ &\mathbb{E}\{|\frac{\frac{1}{M_s}\sum_{m=1}^{M_s}(\mathbf{g}_{m1}^{DF}\text{diag}\{\hat{\mathbf{g}}_{m2}^U\}\epsilon_{F,m}^{-1}\mathbf{w}_m^H)}{\frac{1}{M_s}\sum_{m=1}^{M_s}(\bar{\gamma}_{F,m}\sum_{n=1}^{N_t}|X_{F,m,n}|^2)}|^2\}, \quad \text{(A.4)}
\end{aligned}$$

and

$$\begin{aligned}
&\mathbb{E}\{|1-\frac{\mathbf{u}_F^H {\mathbf{R_F}}^{-1}\mathbf{D}_F\mathbf{u}_F}{\mathbf{u}_F^H {\mathbf{R_F}}^{-1}\mathbf{u}_F}|^2|\mu_{21}|^2\} \\
=\ &\mathbb{E}\{|1-\frac{\sum_{m=1}^{M_s}(\bar{\gamma}_{F,m}\frac{D_{m1}}{D_{m2}}\sum_{n=1}^{N_t}|X_{F,m,n}|^2)}{\sum_{m=1}^{M_s}(\bar{\gamma}_{F,m}\sum_{n=1}^{N_t}|X_{F,m,n}|^2)}|^2|\mu_{21}|^2\} \\
\overset{(b)}{=}\ &\mathbb{E}\{|1-\frac{\frac{1}{M_s}\sum_{m=1}^{M_s}(\bar{\gamma}_{F,m}\frac{\cos\theta_{m1}}{\cos\theta_{m2}}\sum_{n=1}^{N_t}|X_{F,m,n}|^2 e^{-j\Delta\omega_{m2}})}{\frac{1}{M_s}\sum_{m=1}^{M_s}(\bar{\gamma}_{F,m}\sum_{n=1}^{N_t}|X_{F,m,n}|^2)}|^2 \\
&\cdot|\mu_{21}|^2\}, \quad \text{(A.5)}
\end{aligned}$$

where (b) is obtained by substituting $D_{mb} = \cos\theta_{mb} e^{j\Delta\omega_{mb}}$. Note that $\omega_{m1} \triangleq \phi_{m1} - \phi_{m1} = 0$ and $\hat{\omega}_{m1} = \Delta\omega_{m1} = 0$.

Again, from the law of large numbers we have

$$\begin{aligned}&\lim_{M_s\to\infty} \frac{1}{M_s}\sum_{m=1}^{M_s}(\mathbf{g}_{m1}^{DF}\mathrm{diag}\{\hat{\mathbf{g}}_{m2}^{U}\}\epsilon_{F,m}^{-1}\mathbf{w}_m^H)\\ =\ & \mathbb{E}\{\mathbf{g}_{m1}^{DF}\mathrm{diag}\{\hat{\mathbf{g}}_{m2}^{U}\}\epsilon_{F,m}^{-1}\mathbf{w}_m^H\},\end{aligned} \tag{A.6}$$

and

$$\begin{aligned}&\lim_{M_s\to\infty} \frac{1}{M_s}\sum_{m=1}^{M_s}(\bar{\gamma}_{F,m}\frac{\cos\theta_{m1}}{\cos\theta_{m2}}\sum_{n=1}^{N_t}|X_{F,m,n}|^2 e^{-j\Delta\omega_{m2}})\\ =\ & N_t\mathbb{E}\{\bar{\gamma}_{F,m}\frac{\cos\theta_{m1}}{\cos\theta_{m2}}|X_{F,m,n}|^2 e^{-j\Delta\omega_{mb2}}\},\end{aligned} \tag{A.7}$$

and

$$\begin{aligned}&\lim_{M_s\to\infty} \frac{1}{M_s}\sum_{m=1}^{M_s}(\bar{\gamma}_{F,m}\sum_{n=1}^{N_t}|X_{F,m,n}|^2)\\ =\ & N_t\mathbb{E}\{\bar{\gamma}_{F,m}|X_{F,m,n}|^2\}.\end{aligned} \tag{A.8}$$

Substituting (A.6), (A.7), (A.8) and $\mathbb{E}\{|\mu_{21}|^2\} = \bar{\mu}^2$ into (30), the asymptotic MSE of the C-MSC is

$$\begin{aligned}&\lim_{M_s\to\infty}\mathrm{MSE}(\hat{\mu}_{21}^F)\\ =\ & \psi^2+\bar{\mu}^2|1-\frac{\mathbb{E}\{\bar{\gamma}_{F,m}\frac{\cos\theta_{m1}}{\cos\theta_{m2}}|X_{F,m,n}|^2 e^{-j\Delta\omega_{mb2}}\}}{\mathbb{E}\{\bar{\gamma}_{F,m}|X_{F,m,n}|^2\}}|^2,\end{aligned} \tag{A.9}$$

where $\psi = |\frac{\mathbb{E}\{(\mathbf{g}_{m1}^{DF}\mathrm{diag}\{\hat{\mathbf{g}}_{m2}^{U}\}\epsilon_{F,m}^{-1}\mathbf{w}_m^H)\}}{N_t\mathbb{E}\{(\bar{\gamma}_{F,m}|X_{F,m,n}|^2)\}}|$.

Considering the definition of PA difference and the fact that $e^{-j\Delta\omega_{mb2}}$ is independent from the quantization of per-cell channels, we have

$$\begin{aligned}&\mathbb{E}\{\bar{\gamma}_{F,m}\frac{\cos\theta_{m1}}{\cos\theta_{m2}}|X_{F,m,n}|^2 e^{-j\Delta\omega_{m2}}\}\\ =\ & \mathbb{E}\{\bar{\gamma}_{F,m}\frac{\cos\theta_{m1}}{\cos\theta_{m2}}|X_{F,m,n}|^2\}\mathbb{E}\{e^{-j\Delta\omega_{m2}}\}.\end{aligned} \tag{A.10}$$

When uniform quantization is applied to quantize the PA difference, the quantization errors are modeled as random variables uniformly distributed in $[-2^{-B_P}\pi, 2^{-B_P}\pi]$. Then, we have

$$\begin{aligned}\mathbb{E}\{e^{-j\Delta\omega_{m2}}\} &= \int_{-2^{-B_P}\pi}^{2^{-B_P}\pi}\frac{e^{-j\Delta\omega_{m2}}}{2\times 2^{-B_P}\pi}d\Delta\omega_{m2}\\ &= \frac{\sin(2^{-B_P}\pi)}{2^{-B_P}\pi}.\end{aligned} \tag{A.11}$$

Substituting (A.10) and (A.11) into (A.9), we immediately obtain (32).

APPENDIX B
PROOF OF PROP.3

From (34) the MSE of the inter-BS ambiguity factor estimate is

$$\mathrm{MSE}(\hat{\mu}_{21}^T) = \mathbb{E}_{\mathbf{X}}\{(\bar{\gamma}\mathbf{X}^H\mathbf{X})^{-1}\}, \tag{B.1}$$

where $\mathbb{E}\{\mathbf{X}\mathbf{X}^H\} = \mathbf{\Phi}_{\mathbf{X}}$, and $\mathrm{Tr}(\mathbf{\Phi}_{\mathbf{X}}) = M_s$.

Because $\mathbf{\Phi}_{\mathbf{X}}$ is a Hermitian matrix, its eigen-decomposition is $\mathbf{\Phi}_{\mathbf{X}} = \mathbf{U}\mathbf{\Lambda}\mathbf{U}^H$, where $\mathbf{U}$ is a unitary matrix, $\mathbf{\Lambda} = \mathrm{diag}([\lambda_1\cdots\lambda_{M_s}])$ is a diagonal matrix, and $\lambda_1 \geq \cdots \geq \lambda_{M_s} = M_s - \sum_{m=1}^{M_s-1}\lambda_m$.

Denote $\boldsymbol{\xi} = \mathbf{\Lambda}^{-1/2}\mathbf{U}^H\mathbf{X}$. Then, $\boldsymbol{\xi}$ is a complex Gaussian random vector with zero mean and covariance matrix $\mathbf{I}_{M_s}$, the elements of $\boldsymbol{\xi}$ are independent, and $|\xi_m|^2$ follows exponential distribution with parameter 1, whose probability density function is $f(x) = \exp(-x), x \geq 0$.

After these matrix transformations, we can rewrite (B.1) as

$$\begin{aligned}&\mathrm{MSE}(\hat{\mu}_{21}^T)\\ =\ & \frac{1}{\bar{\gamma}}\mathbb{E}\{(\sum_{m=1}^{M_s}\lambda_m|\xi_m|^2)^{-1}\}\\ =\ & \frac{1}{\bar{\gamma}}\iint_0^{+\infty}\frac{\exp(-\sum_{m=1}^{M_s}x_m)}{\sum_{m=1}^{M_s}\lambda_m x_m}dx_1\cdots dx_{M_s}.\end{aligned} \tag{B.2}$$

We can prove that $\mathrm{MSE}(\hat{\mu}_{21}^T)$ is an increasing function of λ_1 by finding the partial derivative as

$$\begin{aligned}&\frac{\partial\mathrm{MSE}(\hat{\mu}_{21}^T)}{\partial\lambda_1}\\ =\ & \frac{1}{\bar{\gamma}}\iint_0^{+\infty}\frac{x_{M_s}-x_1}{(\sum_{m=1}^{M_s}\lambda_m x_m)^2}\exp(-\sum_{m=1}^{M_s}x_m)dx_1\cdots dx_{M_s}\\ =\ & \frac{1}{\bar{\gamma}}\iint_{x_1>x_{M_s}}\frac{x_{M_s}-x_1}{(\sum_{m=1}^{M_s}\lambda_m x_m)^2}\exp(-\sum_{m=1}^{M_s}x_m)dx_1\cdots dx_{M_s}\\ +\ & \frac{1}{\bar{\gamma}}\iint_{x_1<x_{M_s}}\frac{x_{M_s}-x_1}{(\sum_{m=1}^{M_s}\lambda_m x_m)^2}\exp(-\sum_{m=1}^{M_s}x_m)dx_1\cdots dx_{M_s}\\ \overset{(a)}{=}\ & \frac{1}{\bar{\gamma}}\iint_{x_1>x_{M_s}}\frac{x_{M_s}-x_1}{(\sum_{m=1}^{M_s}\lambda_m x_m)^2}\exp(-\sum_{m=1}^{M_s}x_m)dx_1\cdots dx_{M_s}\\ -\ & \frac{1}{\bar{\gamma}}\iint_{x_1'>x_{M_s}'}\frac{(x_{M_s}'-x_1')\exp(-\sum_{m=1}^{M_s}x_m)}{(\lambda_{M_s}x_1'+\sum_{m=2}^{M_s-1}\lambda_m x_m+\lambda_1 x_{M_s}')^2}dx_1'\cdots dx_{M_s}'\\ =\ & \frac{1}{\bar{\gamma}}\iint_{x_1>x_{M_s}}(-\frac{x_{M_s}-x_1}{(\lambda_{M_s}x_1+\sum_{m=2}^{M_s-1}\lambda_m x_m+\lambda_1 x_{M_s})^2}\\ +\ & \frac{x_{M_s}-x_1}{(\sum_{m=1}^{M_s}\lambda_m x_m)^2})\exp(-\sum_{m=1}^{M_s}x_m)dx_1\cdots dx_{M_s},\end{aligned} \tag{B.3}$$

where (a) is a coordinate transformation by setting $x_1' = x_{M_s}$ and $x_{M_s}' = x_1$. When $x_1 > x_{M_s}$ and $\lambda_1 > \lambda_{M_s}$, $\lambda_1 x_1 + \lambda_{M_s}x_{M_s} > \lambda_{M_s}x_1 + \lambda_1 x_{M_s}$, therefore $\frac{x_{M_s}-x_1}{(\sum_{m=1}^{M_s}\lambda_m x_m)^2} > \frac{x_{M_s}-x_1}{(\lambda_{M_s}x_1+\sum_{m=2}^{M_s-1}\lambda_m x_m+\lambda_1 x_{M_s})^2}$, and the term inside the integrals is positive. Then we obtain $\frac{\partial\mathrm{MSE}(\hat{\mu}_{21}^T)}{\partial\lambda_1} > 0$.

It indicates that the decrease of the largest eigenvalue of $\mathbf{\Phi}_{\mathbf{X}}$ will lead to the decrease of the MSE. Therefore, the MSE achieves its minimum if and only if all the eigenvalues are equal, i.e., when the covariance matrix $\mathbf{\Phi}_{\mathbf{X}} = \mathbf{I}$.

REFERENCES

[1] J. Zhang, J. A. R. Chen, A. Ghosh, and R. W. Heath, "Networked MIMO with clustered linear precoding," *IEEE Trans. Wireless Commun.*, vol. 8, pp. 1910–1921, Apr. 2009.

[2] E. Bjornson, R. Zakhour, D. Gesbert, and B.Ottersten, "Cooperative multicell precoding: rate region characterization and distributed strategies with instantaneous and statistical CSI," *IEEE Trans. Signal Process.*, vol. 58, pp. 4298–4310, Aug. 2010.

[3] W. Ho, T. Quek, S. Sun, and R. Heath, "Decentralized precoding for multicell MIMO downlink," *IEEE Trans. Wireless Commun.*, vol. 10, pp. 1798–1809, June 2011.
[4] M. Mazrouei-Sebdani and W. Krzymien, "Vector perturbation precoding for network MIMO: sum rate, fair user scheduling, and impact of backhaul delay," *IEEE Trans. Veh. Technol.*, vol. 61, pp. 3946–3957, Nov. 2012.
[5] T. M. Kim, F. Sun, and A. Paulraj, "Low-complexity MMSE precoding for coordinated multipoint with per-antenna power constraint," *IEEE Signal Process. Lett.*, vol. 20, pp. 395–398, June 2013.
[6] M. K. Karakayali, G. J. Foschini, and R. A. Valenzuela, "Network coordination for spectrally efficient communications in cellular systems," *IEEE Wireless Commun. Mag.*, vol. 13, pp. 56–61, Aug. 2006.
[7] D. Gesbert, S. Hanly, H. Huang, S. S. Shitz, O. Simeone, and W. Yu, "Multi-cell MIMO cooperative networks a new look at interference," *IEEE J. Sel. Areas Commun.*, vol. 28, pp. 1380–1408, Dec. 2010.
[8] X. Hou and C. Yang, "Feedback overhead analysis for base station cooperative transmission," *IEEE Trans. Wireless Commun.*, early access, 2013.
[9] J. Shi, Q. Luo, and M. You, "An efficient method for enhancing TDD over the air reciprocity calibration," in *Proc. 2011 IEEE WCNC.*
[10] M. Guillaud and F. Kaltenberger, "Towards practical channel reciprocity exploitation: relative calibration in the presence of frequency offset," in *Proc. 2013 IEEE WCNC.*
[11] S. Han, L. Su, C. Yang, G. Wang, and M. Lei, "Robust multiuser precoder for base station cooperative transmission with non-ideal channel reciprocity," in *Proc. 2010 IEEE GLOBECOM.*
[12] J. G. F. Huang, Y. Wang, and D. Yang, "Antenna mismatch and calibration problem in coordinated multi-point transmission system," *IET Commun.*, vol. 6, no. 3, pp. 289–299, Feb. 2012.
[13] 3GPP R1-092659, "Antenna calibrations for TDD CoMP," Samsung, 2009.
[14] 3GPP Long Term Evolution (LTE), "Physical Channels and Modulation," TS 36.211 V10.0.0 Release 10, 2011.
[15] ——, "Physical layer procedures," TS 36.213 V10.2.0, 2011.
[16] 3GPP R1- 091752, "Performance study on Tx/Rx mismatch in LTE TDD dual-layer beamforming," Nokia, Nokia Siemens Networks, CATT, ZTE, 2009.
[17] P. H. Moose, "A technique for orthogonal frequency division multiplexing frequency offset correction," *IEEE Trans. Commun.*, vol. 42, no. 10, pp. 2908–2914, 1994.
[18] J. Beek, P. Borjesson, M. Boucheret, D. Landstrom, J. Arenas, P. Odling, C. Ostberg, M. Wahlqvist, and S. Wilson, "A time and frequency synchronization scheme for multiuser OFDM," *IEEE J. Sel. Areas Commun.*, vol. 17, no. 11, pp. 1900–1914, 1999.
[19] 3GPP R1-093542, "Study on channel reciprocity in LTE-A," *CATT*, 2009.
[20] D. Su, X. Hou, and C. Yang, "Quantization based on per-cell codebook in cooperative multi-cell systems," in *Proc. 2011 IEEE WCNC.*
[21] N. Jindal, "MIMO broadcast channels with finite rate feedback," *IEEE Trans. Inf. Theory*, vol. 52, pp. 5045–5059, Nov. 2006.
[22] Y. Kim, "A differential codebook using 8-PSK alphabets for slowly fading channels," *Proc. 2012 IEEE VTC — Fall.*
[23] 3GPP TSG RAN and TR 25.814 v7.1.0, "Physical layer aspects for evolved UTRA," Sept. 2006.
[24] H.Holma and A.Toskala, *LTE for UMTS: OFDMA and SC-FDMA Based Radio Access*. John Wiley and Sons, 2009.
[25] H. Huang, M. Trivellato, A. Hottinen, M. Shafi, P. Smith, and R. A. Valenzuela, "Increasing downlink cellular throughput with limited network MIMO coordination," *IEEE Trans. Wireless Commun.*, vol. 8, pp. 2983–2989, June 2009.
[26] W. Jakes and D. Cox, *Microwave Mobile Communications.* Wiley-IEEE Press, 1994.
[27] D. J. Love, R. W. Heath, and T. Strohmer, "Grassmannian beamforming for multiple-input multiple-output wireless systems," *IEEE Trans. Inf. Theory*, vol. 49, pp. 2735–2747, Oct. 2003.
[28] H. Maattanen, O. Tirkkonen, and T. Roman, "CQI-report optimization for multi-mode MIMO with unitary codebook based precoding," *Proc. 2009 IEEE PIMRC.*
[29] A. Wiesel, Y. Eldar, and S. Shamai, "Zero-forcing precoding and generalized inverses," *IEEE Trans. Signal Process.*, vol. 55, no. 9, pp. 4409–4418, Sep. 2008.
[30] X. Hou, C. Yang, and B. K. Lau, "Impact of non-orthogonal training on performance of downlink base station cooperative transmission," *IEEE Trans. Veh. Technol.*, vol. 60, pp. 4633–4639, Sept 2011.

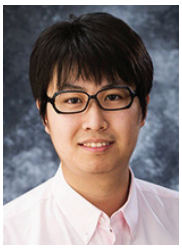

Liyan Su received his B. Eng degree in the School of Advanced Engineering from Beihang University (BUAA), Beijing, China in 2010. He is now pursuing a Ph.D degree in the School of Electronics and Information Engineering from BUAA. His research interests lie in the area of energy efficient and spectral efficient multi-cell MIMO systems.

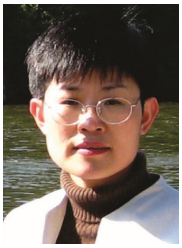

Chenyang Yang (SM'08) received the M.S.E and Ph.D. degrees in electrical engineering from Beihang University (formerly Beijing University of Aeronautics and Astronautics), Beijing, China, in 1989 and 1997, respectively. She is currently a Full Professor with the School of Electronics and Information Engineering, Beihang University. Her recent research interests include green radio, interference coordination and cooperative transmission for large scale networks. Prof. Yang was the Chair of the IEEE Communications Society Beijing chapter from 2008 to 2012. She has served as Technical Program Committee Member for many IEEE conferences. She currently serves as an Associate editor for IEEE TRANSACTIONS ON WIRELESS COMMUNICATIONS, a guest editor of IEEE JOURNAL OF SELECTED TOPICS IN SIGNAL PROCESSING, an Associate Editor-in-Chief of the *Chinese Journal of Communications*, and an Associate editor-in chief of the *Chinese Journal of Signal Processing*. She was nominated as an Outstanding Young Professor of Beijing in 1995 and was supported by the First Teaching and Research Award Program for Outstanding Young Teachers of Higher Education Institutions by Ministry of Education (P.R.C. "TRAPOYT") during 1999-2004.

Gang Wang received the Ph.D. degree from Tsinghua University in 2006. He joined NEC Laboratories China in 2006 and worked on wireless networking. From 2009, he started research on 3GPP LTE standardization. He visited UC Davis in 2011 and worked with Prof. Zhi Ding on CoMP. He is now a senior researcher at NEC Laboratories China. His research interest includes MIMO, CoMP, dynamic TDD system and coverage enhancement.

Ming Lei received the B.Eng. degree from the Southeast University in 1998 and the Ph.D. degree from BUPT (Beijing University of Posts & Telecommunications) in 2003, all in Electrical Engineering. From April 2003 to February 2008, he was a research scientist with the National Institute of Information and Communications Technology (NICT), Japan, where he contributed to Japan's national projects on 4G mobile communications (MIRAI projects) and IEEE standardization of 60-GHz multi-gigabit WPAN (IEEE 802.15.3c). From March 2008 to May 2009, he was a project lead of Intel Corporation, where he contributed to the standardization of WiGig (60-GHz WPAN), IEEE 802.11ad (60-GHz WLAN) and IEEE 802.16m (mobile WiMAX). Since May 2009, he has been with NEC Laboratories China, NEC Corporation, as the department head managing the wireless research and standardization projects on 4G cellular mobile communications (LTE and LTE-Advanced), 60-GHz, mobile backhaul, etc. Dr. Ming Lei was elected to IEEE Senior Member in 2009.